

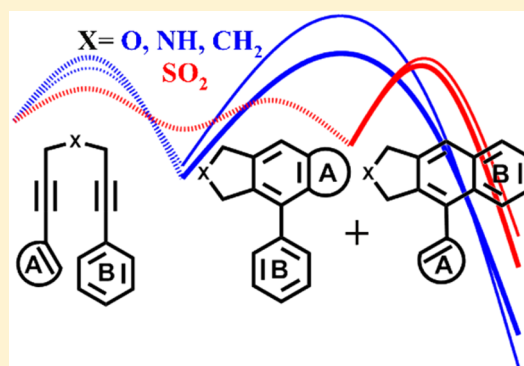
# Does the Mechanism of the Garratt–Braverman Cyclization Differ with Substrates? A Computational Study on Bispropargyl Sulfones, Sulfides, Ethers, Amines, and Methanes

Saibal Jana and Anakuthil Anoop\*

Department of Chemistry, Indian Institute of Technology Kharagpur, Kharagpur 721 302, India

**S** Supporting Information

**ABSTRACT:** We studied the variation in mechanism among different bispropargyl substrates—sulfone, sulfide, ether, amine, and methane—toward Garratt–Braverman (GB) cyclization using density functional theory calculations. Isomerization and cycloaddition are the key steps in the GB cyclization. To compare the reactivity among the various substrates, we computed the free energy of activation ( $\Delta G^\ddagger$ ) for the cycloaddition and the cyclization steps, whereas we used the theoretically computed  $pK_a$  values for the isomerization steps. Our results suggest that the sulfones undergo a relatively fast isomerization followed by slower cyclization, while the ethers undergo a slow isomerization followed by easy cyclization. The methanes and amines are similar to the ethers, and the sulfides showed intermediate behavior. We extended our study to unsymmetrical substrates and compare the results with experiments that suggest the isomerization to be the rate-limiting step for bispropargyl ethers, while cyclization through a diradical intermediate is crucial to the rate for the bispropargyl sulfones. On the basis of these findings, we made predictions on the selectivity of unsymmetrical bispropargyl sulfones, amines, methanes, and sulfides. This is the first detailed mechanistic study on the GB cyclization of bispropargyl substrates other than sulfones.

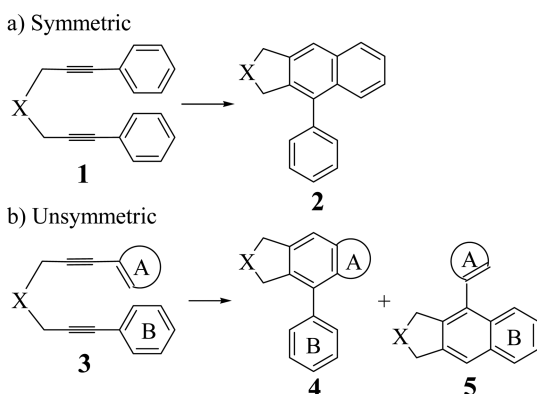


## INTRODUCTION

A type of thermal cyclization involving bispropargyl compounds, Garratt–Braverman (GB) cyclization (Scheme 1), is a fascinating problem for mechanistic studies. The base-catalyzed cyclization of bispropargyl sulfones, sulfides, and ethers reported individually by Garratt et al.<sup>1,2</sup> and Braverman et al.<sup>3,4</sup> is an efficient route to synthesize various polycyclic

aromatic compounds of biological interest. The mechanism of the GB cyclization involves three basic steps:<sup>5–8</sup> (1) base-mediated isomerization of alkyne to allene, (2) cyclization via a diradical intermediate, and (3) aromatization through H-rearrangements. There is only one variation proposed in this major route, namely, [4 + 2] cycloaddition from an allenyne intermediate.<sup>9</sup> Selectivity of GB cyclization of unsymmetrical substrates<sup>6,10</sup> is even more exciting for synthetic chemists as a route to complex biologically important molecules, but at the same time the increased complexity is challenging for theoretical studies.

**Scheme 1. Garratt–Braverman Cyclization of Bispropargyl Substrates: (a) Symmetric and (b) Unsymmetric Systems<sup>a</sup>**



<sup>a</sup>Here, X is a linker (SO<sub>2</sub>, O, CH<sub>2</sub>, S, and NH). A and B inside the ring designate the asymmetry of the systems (see Table 1 or Scheme 3).

Our current interest in this reaction is driven by a few experimental observations that suggested plausible variations in the mechanism when any of the following modifications are made to the parent substrate: changing the linker group (X) (Scheme 1) connecting two propargyl groups, making substitutions in the phenyl rings, or replacing the phenyl groups with heteroaromatic rings. Basak and co-workers<sup>11</sup> recently reported selectivity with GB cyclization of unsymmetrical bispropargyl ethers. Two products are possible, depending on which of the aromatic rings participates selectively during the new six-membered-ring formation. They also suggested that bispropargyl ethers may go through a mechanism different from that of the sulfones. These

Received: May 5, 2016

Published: July 27, 2016

experimental findings provided key information for us in our study of some important aspects of the mechanism of GB cyclization.

In this work, we have explored various pathways in the mechanisms for symmetric bispropargyl sulfone, ether, methane, sulfide, and amine, where the atom/group that links the two propargyl units is SO<sub>2</sub>, O, CH<sub>2</sub>, S, and NH, respectively. In the unsymmetrical substrates, understanding the factors controlling the selectivity is important. To address this, we have investigated the mechanistic origin of selectivity in the cyclization of unsymmetrical bispropargyl ethers as the test system and compared the results with the experimentally reported selectivity. We have included all the reported<sup>11</sup> combinations of aryl/heteroaryl substituents at the acetylene termini of bispropargyl ether. After establishing the origin of selectivity, we studied similar substrates, namely, bispropargyl sulfones, sulfides, methanes, and amines, and made predictions of their selectivity in the GB cyclization.

## COMPUTATIONAL DETAILS

All the geometry optimizations and free energy calculations for symmetric and unsymmetric systems were made using density functional theory with the def2-SVP<sup>12</sup> basis set. Empirical dispersion correction (D3<sup>13</sup>) is included to account for noncovalent interactions. The resolution of identity (RI)<sup>14</sup> approximation with corresponding auxiliary basis sets was employed to speed up the calculations. In general, DFT-D3 provides fairly good accuracy comparable to the wave-function-based methods for practical purposes.<sup>15</sup> Hybrid functionals in general give better results, but pure GGA functionals (BP86, BPW91<sup>13,16</sup>) are also shown to perform well for the diradical systems.<sup>17</sup> We have compared the results with single-point evaluations at BP86-D3/def2-TZVP, BPW91/def2-SVP, BPW91/def2-TZVP, B3LYP-D3/def2-TZVP,<sup>18–20</sup> M06-2X/def2-SVP, and M06-2X/def2-TZVP levels for a set of reactions, and the results are provided in the [Supporting Information](#). The closed-shell species are calculated with the restricted formalism, and the open-shell species are treated with the broken-symmetry approach. The reported energies (electronic and free energies) are taken from the optimization with the M06-2X<sup>21</sup> functional for the symmetric systems and from the less expensive BP86<sup>22,23</sup> functional for the asymmetric systems. Frequency calculations were carried out, and the stationary points are characterized by vibrational frequency calculations. All the optimized geometries have no imaginary mode, except the transition-state geometries, which have only one imaginary mode. The transition states were analyzed, and it was verified that they belong to the corresponding steps by the visual inspection of the imaginary mode and also by the free optimization of the coordinates transformed along the mode of reaction. To understand the nature of diradical intermediates, spin density plots were generated, which showed considerable spin density on the carbon centers (Figure S2, [Supporting Information](#)). The solvent effect was taken into account during optimization and the free energy calculation using COSMO<sup>24–27</sup> solvation model implemented in Orca, with THF as the solvent. All calculations were done with the Orca 2.9.1 and Orca 3.0.0 software packages.<sup>28</sup>

Approaches in theoretical pK<sub>a</sub> calculations are based on the use of thermodynamic cycles (Figure 1).<sup>29</sup> In the cycles, gas-phase deprotonation free energies ( $\Delta G_{\text{gas}}$ ) and solvation free energies ( $\Delta G_{\text{solv}}$ ) of the involved species were used to calculate the free energy of deprotonation in solution ( $\Delta G_{\text{soln}}$ ). Solution-

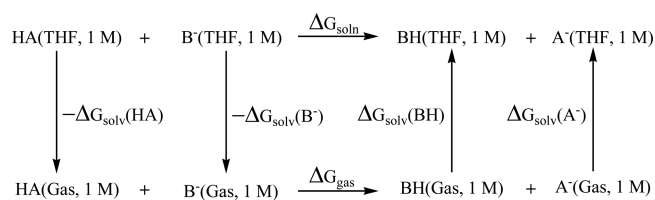


Figure 1. Thermodynamic cycle used in the calculation of pK<sub>a</sub>.

phase free energies were calculated from the dielectric continuum models. Among the number of thermodynamic cycles in use, we chose the proton exchange method (also called isodesmic method).

The calculated pK<sub>a</sub> by this method is a relative pK<sub>a</sub>. It is more reliable than the direct pK<sub>a</sub> calculation due to the conservation of charged species on both sides of the equation. Additionally, this approach has the advantage of further cancellation of errors from lower levels of theory and errors in a continuum model and in gas-phase reaction energies. The pK<sub>a</sub> can be obtained from the following equations:

$$\text{pK}_a = \frac{\Delta G_{\text{soln}}}{RT \ln(10)} + \text{pK}_a(\text{BH}) \quad (1)$$

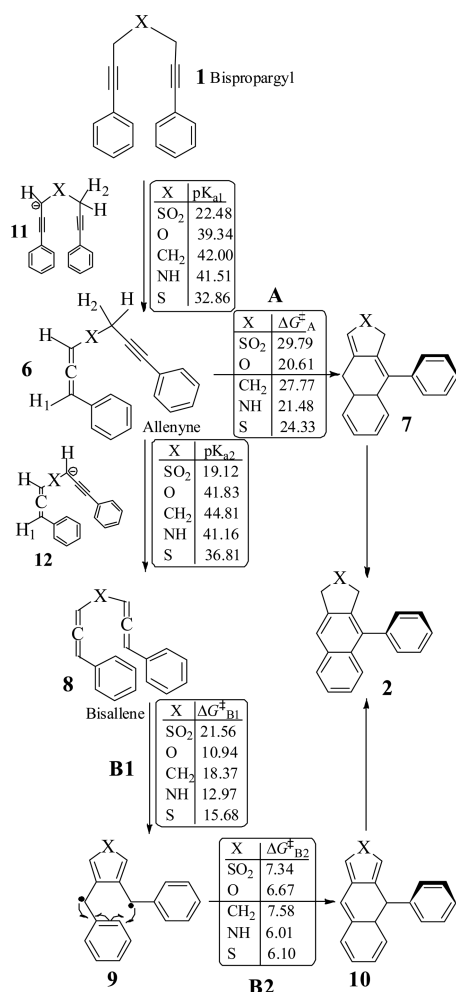
$$\Delta G_{\text{soln}} = \Delta G_{\text{gas}} + \sum_{i=1}^{N_{\text{products}}} n_i \Delta G_{\text{solv},i} - \sum_{j=1}^{N_{\text{reactants}}} n_j \Delta G_{\text{solv},j} \quad (2)$$

To avoid the calculation of  $\Delta G_{\text{solv}}(\text{H}^+)$  that is required in many thermodynamic cycles, the experimental pK<sub>a</sub> of a reference base (BH) was used. The pK<sub>a</sub> calculated by this method is dependent on the reference. Best results are obtained when the reference (BH) is similar to the molecule under investigation and the pK<sub>a</sub> is determined in the same solvent. However, in this work we compared the calculated pK<sub>a</sub> among the systems under study, and no reference is made with the experimental pK<sub>a</sub>; therefore, the choice of reference is not critical. We used diphenylmethane (pK<sub>a</sub> = 35.9)<sup>30</sup> in THF as the reference.

## RESULTS AND DISCUSSION

The details of the elementary steps in the mechanism of GB cyclization are not fully known. A few possible pathways can be proposed based only on the observed products;<sup>31</sup> no intermediates have been isolated yet. Among the basic steps mentioned in the [Introduction](#), the final aromatization through H-rearrangements is assumed to be less crucial to the rate or selectivity once the cyclization is completed. We have computed activation free energies for the following cyclization steps (Scheme 2): (A) intramolecular Diels–Alder cycloaddition (IMDA) (allenyne → cyclized intermediate), (B1) first cyclization (bisallene → diradical intermediate), and (B2) second cyclization (diradical → cyclized intermediate). Corresponding activation free energies are represented as  $\Delta G_{\text{A}}^\ddagger$ ,  $\Delta G_{\text{B1}}^\ddagger$ , and  $\Delta G_{\text{B2}}^\ddagger$  (kcal mol<sup>-1</sup>), respectively.

Computing the activation energy for the isomerization was, however, not easy, as the transition state for the alkyne–allene isomerization was elusive. Theoretical studies recorded in the literature are few.<sup>32</sup> The basic steps are the abstraction of H from the propargyl position by a base and the return of the H (the same or another H) to the allenyl anion. To compare the rate of isomerization among similar species, a good approximation is to estimate the energy required to break the

Scheme 2. [4 + 2] IMDA Cycloaddition and Diradical Mechanism of GB Cyclization<sup>a</sup>

<sup>a</sup>The pK<sub>a</sub> corresponding to alkyne–allene isomerization and activation free energies (at M06-2X/def2-SVP level, in kcal mol<sup>-1</sup>) for cyclization steps are given. These activation energies are the stepwise activation free energies, calculated as the difference in free energy between the transition state and the previous intermediates or reactants in the corresponding pathways.

corresponding propargyl C–H bond. A suitable parameter here that is also appealing to the experimentalists is the pK<sub>a</sub> of the propargyl hydrogen. We have calculated the pK<sub>a1</sub> and pK<sub>a2</sub> corresponding to the first and second isomerization using the method described in the [Computational Details](#) section.

**GB Cyclization of Symmetric Bispropargyl Substrates (1, X = SO<sub>2</sub>, O, CH<sub>2</sub>, S, and NH).** Bispropargyl sulfones (1, X = SO<sub>2</sub>) are the most studied system experimentally and theoretically, and results indicate that they are unique in many respects. For sulfones, the intermediates after the isomerization, allenyne (6, X = SO<sub>2</sub>) and bisallene (8, X = SO<sub>2</sub>), are almost isoenergetic with the bispropargyl substrates. In all other cases, allenyne (6) is more stable than bispropargyls (1), and bisallenes (8) are even more stable than allenyne (6) (Figure 2). In general, allenes are less stable than alkynes; however, in our allenyne and bisallene systems, the π–π interaction between the phenyl groups at the terminal positions leads to an extra stability.<sup>33</sup> The phenyl groups in the bispropargyls do not enjoy the stability of a π–π interaction, as the repulsive interaction between the alkynyl groups forces the phenyl

groups to stay away from each other. The alkyne–allene isomerization provides flexibility to the phenyl groups to maintain a conformation that is suitable for π–π interaction. Thus, allenyne and bisallenes are more stable than the bispropargyls (except for 8, X = SO<sub>2</sub>). Moreover, allenyne and bisallenes (6 and 8, X = NH, O, S) also enjoy stabilization from an extended conjugation of their allenyl π-orbitals with the p-orbital of the heteroatoms in the amine, ether, and sulfide. Methane is also slightly stabilized by hyperconjugation. The hyperconjugative effect can be seen in the bond shortening in C–X bonds (Table S4 in the [Supporting Information](#)). Hence the amines gain maximum stabilization by isomerization, followed by ether, sulfides, and methanes, respectively.

The stabilization by conjugation also results in the stabilization of the diradical intermediates (9) when X = NH, O, and S. The five-membered rings formed by the cyclization of bisallenes are aromatic in these systems. The newly formed C–C bond distances are 1.46–1.47 Å, which support the aromatic character of the bond. On the other hand, the C–C distance is 1.52 Å in 8, X = SO<sub>2</sub>, and 1.507 Å in 8, X = CH<sub>2</sub>, which are closer to the C–C single bond distances. Thus, the aromatic stabilization makes the diradical species even more stable than the closed-shell bisallenes (8). The stabilization on going from 8 to 9 are 25.16 kcal mol<sup>-1</sup> for X = NH, 20.54 kcal mol<sup>-1</sup> for X = O, 19.29 kcal mol<sup>-1</sup> for X = S, and 2.58 kcal mol<sup>-1</sup> for X = CH<sub>2</sub>. Only for sulfone (X = SO<sub>2</sub>), where there is no aromatic stabilization, 9 is less stable than 8.

Taking pK<sub>a</sub> as the appropriate indicator for the favorability of alkyne–allene isomerization, the sulfone with the lowest pK<sub>a1</sub> (22.48) should undergo isomerization most easily (from 1 to 6), followed by sulfide (pK<sub>a1</sub> = 32.86). Ether, amine, and methane have almost similar values for pK<sub>a1</sub> (39.34, 41.51, and 42.00). Similarly, for the second isomerization (from 6 to 8), pK<sub>a2</sub> is the lowest for sulfones. This trend can be attributed to the electron-withdrawing nature of the sulfone moiety. Thus, sulfone undergoes isomerization much more easily than the other substrates in this study.

The sulfone is also unique in having its pK<sub>a1</sub> higher than its pK<sub>a2</sub>. Thus, the second isomerization to bisallene (8, X = SO<sub>2</sub>) from allenyne (6, X = SO<sub>2</sub>) is easier than the formation of allenyne (6, X = SO<sub>2</sub>) from bispropargyl (1, X = SO<sub>2</sub>). Therefore, once allenyne (6, X = SO<sub>2</sub>) is formed, formation of bisallene (8, X = SO<sub>2</sub>) is expected to be facile for the sulfone. For amine, both pK<sub>a</sub> values are almost equal. For methane, sulfide, and ether, the second pK<sub>a</sub> is higher than the first. This implies that the first isomerization to the allenyne from bispropargyl is easier than the second isomerization for methane, sulfide, and ether. Consequently, the allenyne intermediates may have a relatively longer lifetime compared to that of the sulfone and may undergo processes other than the diradical mechanism, namely, IMDA.

The most studied mechanism is the one involving diradical intermediate (the B pathway in Scheme 2). This involves two consecutive C–C bond formations. The barrier for the first cyclization (ΔG<sup>‡</sup><sub>B1</sub>) follows the order sulfone > methane > sulfide > amine > ether. The resulting diradical intermediate (9) forms an aromatic ring for X = S, O, and NH, but not for X = SO<sub>2</sub> or CH<sub>2</sub>, and hence, the barriers are relatively higher for sulfone and methane. The barrier for the first cyclization (ΔG<sup>‡</sup><sub>B1</sub>) is higher than that of the second in all the cases. The reactive diradical intermediate (9) prefers to undergo second cyclization rapidly. ΔG<sup>‡</sup><sub>B1</sub> for X = O is almost half that of the sulfone (X = SO<sub>2</sub>).

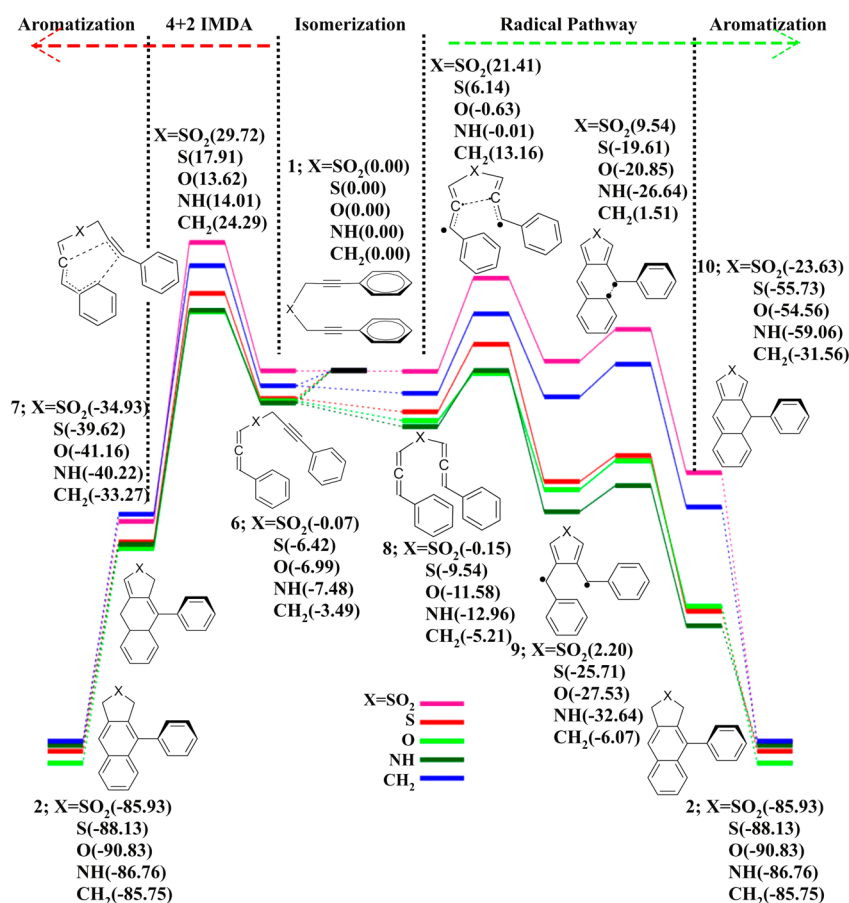


**Figure 2.** Reaction profile for the GB cyclization of symmetric bispropargyl systems through the different mechanisms shown in Scheme 2. The free energy of bispropargyl systems is considered as the reference energy for each system in the reaction profile. Energies (in kcal mol<sup>-1</sup>) are from the M06-2X/def2-SVP level. The solid lines represent the continuous energy profile, where the corresponding transition states are calculated, and the dotted lines connect the intermediates, where the transition states between them are not calculated.

The IMDA (path A) is the cycloaddition between the alkyne as a dienophile and the C=C bond of the aromatic ring and one of the C=C bonds of the allene as the dienes. Activation free energies for the cycloaddition ( $\Delta G_A^\ddagger$ ) of 6, X = SO<sub>2</sub> and CH<sub>2</sub>, are highest, followed by X = S, NH, and O, respectively (Scheme 2). In each case, the barriers are lower for the diradical mechanism (path B) compared to IMDA (path A) (Figure 2).

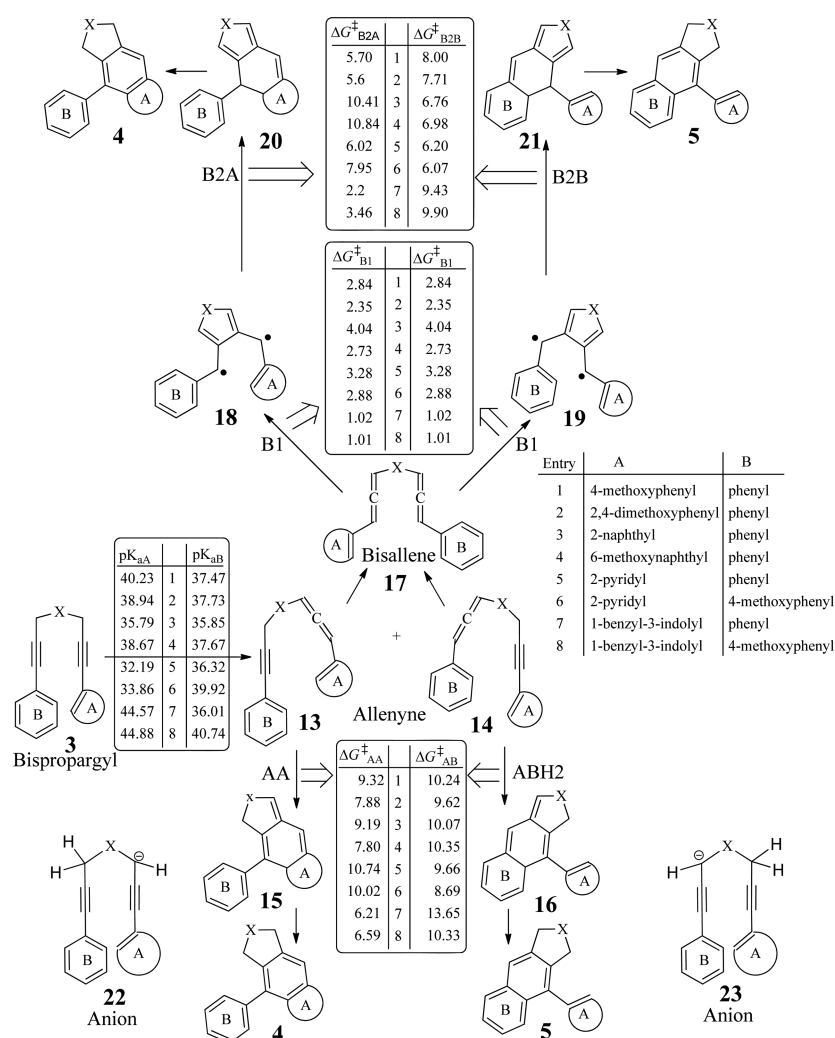
Considering the following scenario and since the barriers for the isomerization are not available, we propose the preferred pathway as follows. If both the isomerizations are easy, then the cyclization will occur from the bisallene intermediate via the diradical mechanism. If the isomerization is difficult, and especially when the second isomerization is more difficult than the first, the cycloaddition can occur from the allenyne intermediate. As both pathways lead to the same product, it is not possible to decide which path occurs from the experiments, besides there is no spectroscopic evidence for a diradical intermediate.

**GB Cyclization of Unsymmetrical Bispropargyl Ethers (X = O).** Unsymmetrical bispropargyl substrates can yield two products, depending on which ring (Scheme 1b) becomes part of the newly formed aromatic ring in the GB cyclization. Previously reported studies on sulfones have shown that the aromatic ring with greater electron density takes part in the cyclization. This is supported by the computed energy barriers for the cyclization through the diradical mechanism. Here, we try to explain the recently reported selectivity<sup>11</sup> in the GB

cyclization of bispropargyl ether (X = O) by comparing the possible mechanisms elucidated above for the symmetric substrates. We studied IMDA (A pathway) and diradical (B pathway) mechanisms and computed the barriers for each step. Scheme 3 contains a schematic representation of the pathways and the relevant barriers and pK<sub>a</sub> values. We have considered eight unsymmetrical bispropargyl ethers (3.1–3.8; Table 1) in this study.

As the number of calculations in the study of unsymmetric bispropargyls is fairly large, we switched the functional to a less expensive pure GGA functional, BP86, after comparing the activation energies for the cycloaddition and cyclization steps for the symmetric systems (section 1.8 in Supporting Information). Although the barriers are higher with the M06-2X functional compared to the barriers from the BP86-D3 functional, the preference for the major pathway among the competing ones is reproduced by both functionals. In these calculations of the symmetric systems, all the geometries were fully optimized in respective methods. In addition, we have also done single-point energy evaluations to compare more functionals and basis sets (section 2.2 in the Supporting Information).

**The Diradical Mechanism.** The first cyclization (path B1) is common for both regioisomeric pathways. The substrate 3.1 (Table 1) has 4-methoxyphenyl (A) and phenyl (B) as the aromatic units. The first barrier ( $\Delta G_{B1}^\ddagger$ ) in the diradical pathway is 2.84 kcal mol<sup>-1</sup> at the BP86/def2-SVP level of

Scheme 3. Two Mechanisms, Diradical (top) and [4 + 2] Cycloaddition (bottom), for the Radical Cyclization of Unsymmetrical Bispropargyl Substrates<sup>a</sup>

<sup>a</sup>The  $pK_a$  values correspond to isomerization, and the activation energies (BP86-D3/def2-SVP; kcal mol<sup>-1</sup>) are for entries 3.1–3.8 in Table 1. These activation energies are the relative free energies with respect to the immediate reactants.

Table 1. Unsymmetric Bispropargyl Substrates in Our Study

entry	compound	substitution	
		A	B
1	3.1	4-methoxyphenyl	phenyl
2	3.2	2,4-dimethoxyphenyl	phenyl
3	3.3	2-naphthyl	phenyl
4	3.4	6-methoxynaphthyl	phenyl
5	3.5	2-pyridyl	phenyl
6	3.6	2-pyridyl	4-methoxyphenyl
7	3.7	1-benzyl-3-indolyl	phenyl
8	3.8	1-benzyl-3-indolyl	4-methoxyphenyl

theory. This barrier for a symmetric system was 10.94 kcal mol<sup>-1</sup> ( $\Delta E_{B1}^\ddagger$ , X = O) at the M06-2X/def2-SVP level and 3.30 kcal mol<sup>-1</sup> at the BP86-D3/def2-SVP level. This difference is a

general trend: the barriers from hybrid functionals are higher than the barriers from pure functionals. A similar trend is found for the energy barriers of IMDA also. See sections 1.8 and 2.2 in the Supporting Information for a comparison of the methods. The diradical intermediate (18.1 and 19.1) from this step can cyclize through association of either ring A or ring B. The required energy barriers are  $\Delta G_{B2A}^\ddagger = 5.70$  kcal mol<sup>-1</sup> and  $\Delta G_{B2B}^\ddagger = 8.00$  kcal mol<sup>-1</sup>. Hence, path B2A has a lower barrier and leads to the major product (4) with ring A in the newly formed ring. This is in contrast to the experimental observation that has a 1:8 ratio of A to B.

Adding one more methoxy group to the previous substrate is expected to alter the electron distribution, where the ring A is 2,4-dimethoxyphenyl (3.2) (Table 1). In this case,  $\Delta G_{B1}^\ddagger$  for the first C–C bond formation is reduced by 0.5 kcal mol<sup>-1</sup> compared to that of the previous substrate (3.1) (2.35 kcal mol<sup>-1</sup> vs 2.84 kcal mol<sup>-1</sup>), but the difference between the activation energies for the two pathways, corresponding to cyclization through ring A and ring B, is close to that of 3.1 (Table 1; 2.30 kcal mol<sup>-1</sup> vs 2.11 kcal mol<sup>-1</sup>). Here also the barriers for the second cyclization favor the formation of a product with A in the newly formed ring. Once again, the

Table 2. Computed  $pK_a$ 's for the Bispropargyl Ethers (3, X = O) and Selectivity of the Products Observed in the Experiment

entry	substrate	substitution		$pK_{aA}$	$pK_{aB}$	expt (A:B)
		A	B			
1	3.1	4-methoxyphenyl	phenyl	40.23	37.47	1:8
2	3.2	2,4-dimethoxyphenyl	phenyl	38.94	37.73	1:8
3	3.3	2-naphthyl	phenyl	35.79	35.85	1.6:1
4	3.4	6-methoxynaphthyl	phenyl	38.67	37.67	1:1.25
5	3.5	2-pyridyl	phenyl	32.19	36.32	only A
6	3.6	2-pyridyl	4-methoxyphenyl	33.86	39.92	only A
7	3.7	1-benzyl-3-indolyl	phenyl	44.57	36.01	only B
8	3.8	1-benzyl-3-indolyl	4-methoxyphenyl	44.88	40.74	1:4

Table 3. Energy Difference ( $\Delta E = E_{(\text{anion A})} - E_{(\text{anion B})}$ , kcal mol<sup>-1</sup>) between Two Isomeric Anions<sup>a</sup>

entry	substitution		X			
	A	B	O	CH <sub>2</sub>	NH	S
1	4-methoxyphenyl	phenyl	3.76	4.63	5.62	6.15
2	2,4-dimethoxyphenyl	phenyl	1.66	6.02	6.76	4.13
3	2-naphthyl	phenyl	-0.08	-2.05	0.00	0.03
4	6-methoxynaphthyl	phenyl	1.35	-0.05	1.42	5.51
5	2-pyridyl	phenyl	-5.64	-6.63	-6.51	-3.24
6	2-pyridyl	4-methoxyphenyl	-8.28	-8.77	-8.69	-6.26
7	1-benzyl-3-indolyl	phenyl	11.68	10.92	9.84	10.60
8	1-benzyl-3-indolyl	4-methoxyphenyl	5.65	5.02	5.87	3.41

<sup>a</sup>Calculations were performed at the BP86-D3/def2-SVP level of theory.

experimental result contradicts theory. Similar disagreement between the experimental outcome and theoretical prediction occurs for the substrates 3.3, 3.6, and 3.7. Although theory predicts experimental selectivity in 3.4 and 3.5, the experimental ratios are too small to account for the difference in the barriers. Thus, in all cases, the diradical mechanism does not match the experimental observations. Thus, an alternative mechanism may be in action.

**The IMDA Mechanism.** The alternative mechanism, where the allenyne intermediate formed in the first isomerization undergoes a [4 + 2] IMDA cycloaddition, was considered next. Depending on which triple bond is involved, there are two possible allenyne intermediates. Cycloaddition from each of these intermediates results in a different product. We have calculated and compared the activation free energies for the cycloaddition steps (pathways referred to as AA and AB in Scheme 3). For 14.1–14.4, 14.7, and 14.8, the barriers for the pathway leading to the product (4) with the participation of ring A,  $\Delta G_{AA}^\ddagger$  is lower than the barrier  $\Delta G_{AB}^\ddagger$  for the formation of product 5 from 15. For the substrates 3.5 and 3.6,  $\Delta G_{AA}^\ddagger$  is higher than  $\Delta G_{AB}^\ddagger$ . Except for 3.3, the selectivity predicted from the activation free energies contradicts the experimentally observed selectivity (Table 2). Hence, predictions based on the IMDA pathway also fail to explain the experimental results.

A possible reason for the deviation of the experimental selectivity from the calculated one is that selectivity may be determined at a different stage of the reaction. In the computational studies on sulfones reported so far, it has been assumed that the rate and selectivity are controlled by the cyclization steps. For the ethers in this study, however, the control of selectivity is not determined by cyclization. A close look at the experimental conditions of the reaction of sulfones and ethers shows that reactions of ethers require higher temperature (reflux),<sup>11</sup> compared to the room-temperature reaction of the sulfones. Yet, the barriers computed for the

ethers are lower than those of the sulfones. This implies that the isomerization could be the rate-limiting step, and the allenyne formed with higher selectivity reacts to form the product in higher yield.

As we did for the symmetric substrates (1), we qualitatively predict the relative rates of isomerization from the relative  $pK_a$ 's of two different propargylic hydrogens. The hydrogen with lower  $pK_a$  is the more acidic and the alkenyl group adjacent to it will isomerize first. If the H adjacent to ring A is the most acidic, then isomerization at the side of the A ring will take place first, and this allenyne will undergo IMDA to form a product with ring A as part of the newly formed aromatic ring. This selectivity predicted from the  $pK_a$  values is in excellent agreement with the experiment. This clearly indicates that the rate of isomerization determines the selectivity for bispropargyl ethers.

**Predicting the Selectivity for the GB Cyclization of Unsymmetric Bispropargyl Amines, Sulfides, and Methanes (X = NH, S, and CH<sub>2</sub>).** Previous studies on bispropargyl sulfones and this study on bispropargyl ethers point to a different behavior for sulfones and ethers: sulfones react through a diradical mechanism and ethers react through IMDA. To predict the selectivity of amines, sulfides, and methanes, we classified them as "sulfone-like" or "ether-like". Unsymmetrical sulfones are compared alongside the other substrates. As we have seen for the symmetric substrates, the  $pK_a$  for bispropargyl sulfone (1, X = SO<sub>2</sub>) is much smaller compared to that of other substrates (1, X = S, O, CH<sub>2</sub>, and NH; see the Supporting Information); the isomerization step of the bispropargyl sulfone could occur at a higher rate than for the others. Thus, the selectivity will be controlled by the rate of cyclization rather than the rate of isomerization.

As the methanes and amines have  $pK_a$  values comparable to those of the ethers, they are expected to follow a mechanism similar to the ethers with selectivity based on the rate of isomerization. The  $pK_a$  values of sulfides lies between those of

**Table 4. Relative Activation Barrier ( $\Delta\Delta G_{B2}^\ddagger = \Delta\Delta G_{B2A}^\ddagger - \Delta\Delta G_{B2B}^\ddagger$ ) between the Two Cyclization Pathways and the Energy Difference between Two Isomeric Anions ( $\Delta E = E_{(\text{anion A})} - E_{(\text{anion B})}$ ) for Unsymmetrical Bispropargyl Sulfones<sup>a</sup>**

entry	substitution		$\Delta\Delta G_{B2}^\ddagger$	$\Delta E$	major products based on	
	A	B			$\Delta\Delta G_{B2}^\ddagger$	$\Delta E$
1	4-methoxyphenyl	phenyl	-1.81	4.13	A	B
2	2,4-dimethoxyphenyl	phenyl	-2.08	4.13	A	B
3	2-naphthyl	phenyl	4.67	0.12	B	B
4	6-methoxynaphthyl	phenyl	4.29	3.06	B	B
5	2-pyridyl	phenyl	-0.45	-6.75	A	A
6	2-pyridyl	4-methoxyphenyl	1.47	-4.71	B	A
7	1-benzyl-3-indolyl	phenyl	-6.61	3.26	A	B
8	1-benzyl-3-indolyl	4-methoxyphenyl	-4.10	0.35	A	B

<sup>a</sup>Calculations were performed at the BP86-D3/def2-SVP level of theory. Energies are in kcal mol<sup>-1</sup>.

sulfone and the methane, ether, and amine. Hence, it is difficult to predict which step determines the selectivity.

The relative  $pK_a$  of the two propargylic H's dictates the energy difference between the two propargyl anions (**22**, **23**; Scheme 3). These differences in energies ( $\Delta E = E_{(\text{anion A})} - E_{(\text{anion B})}$ ) are listed in Tables 3 and 4. In entries 1, 2, 7, and 8, the anion near ring A is more stable for all the substrates (Scheme 3; anion **23**, X = O, CH<sub>2</sub>, NH, S, and SO<sub>2</sub>). In general, the  $\Delta E$ 's are large in the above systems. Conversely, the anion near ring B (**22**, Scheme 3) is more stable in entries 5 and 6 and shows a relatively large energy differences. For the substrates **3.3** and **3.4**, where ring A is naphthyl and 6-methoxynaphthyl, the trend in  $\Delta E$ 's is not clear. Both anions are nearly isoenergetic in entry 3 for all the linkers except for CH<sub>2</sub>. In entry 4, except for CH<sub>2</sub> linker,  $\Delta E$  is positive and so the anion near ring A is more stable. We can translate the above energy differences into the predicted product obtained in major yield when the rate of isomerization determines selectivity. When anionic position is adjacent to ring B,  $\Delta E$  is positive. Positive values in Table 3 represent the product that has the ring B in the polycyclic skeleton and vice versa.

#### Predicting Selectivity for Bispropargyl Sulfones.

According to the arguments outlined above, sulfones are expected to follow a selectivity based on the activation barrier for cyclization rather than the  $pK_a$  value. Thus, we have computed the barriers for extending our prediction to sulfones. Table 4 provides the relative activation barrier between the two cyclization pathways through the diradical mechanism. The relative energies between the respective anions are also given, and these show the prediction based on the rate of isomerization. The predictions on selectivity based on the two criteria generally contradict each other. Therefore, real verification has to come from experiment.

## CONCLUSIONS

We have studied two pathways for GB cyclization—the intramolecular Diels–Alder cycloaddition (IMDA) and the diradical mechanism—first considering symmetric bispropargyl substrates (sulfone, ether, methane, sulfide, and amine) to understand the variation in the mechanisms among these substrates. The  $pK_a$  values of the propargylic hydrogens were estimated theoretically by the proton exchange method, and these were used to predict the relative rates of isomerization. The results show that of these substrates sulfones most easily undergo isomerization because of the relatively high acidity of the propargyl hydrogens. Bispropargyl sulfide followed next in terms of acidity, and the others showed much lower acidity among the systems under study. To compare the two

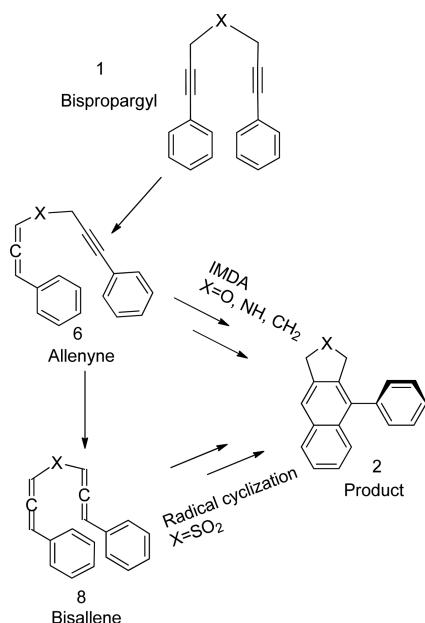
cyclization pathways, we have computed the activation barriers for IMDA and the two cyclization steps in the biradical pathway. The relative activation barriers show that sulfone has the highest barrier for the first cyclization in both the diradical pathway and the IMDA pathway among the substrates we have studied. Methane showed the next highest barrier in the cyclization steps, while the others (ether, sulfide, and amine) have relatively lower barriers. In all these cases, the second cyclization in the diradical pathway has a much lower barrier than the first cyclization.

Unsymmetrical bispropargyl ethers that have experimentally known selectivity were studied in detail for the same pathways as the symmetric substrates. The selectivities predicted from the relative free energies of activation along both of the cyclization pathways are not in agreement with the experimental observation. The alternative possibility, that the relative rate of isomerization controls the selectivity, was examined by calculating the  $pK_a$ 's of the requisite propargyl hydrogens. In this alternative pathway, the propargyl group with the most acidic H undergoes fast isomerization to the corresponding allenyne that goes through IMDA to the respective major product in higher yield. Here, the second isomerization to bisallene will be a less favorable pathway for the formation of the minor product. The relative  $pK_a$ 's in this case of bispropargyl ethers predict the major product in excellent agreement with the experiment.<sup>11</sup>

Thus, the selectivity of the GB cyclization of bispropargyl ethers (X = O) can only be explained by the IMDA pathway, whereas the selectivity in bispropargyl sulfones (X = SO<sub>2</sub>) have been explained<sup>6,10</sup> by the diradical mechanism. While bispropargyl ethers have higher  $pK_a$  values and relatively low cyclization barriers compared to those of sulfones, the rate of isomerization controls the selectivity, whereas the bispropargyl sulfones have low  $pK_a$  values and relatively higher cyclization barriers, and hence the selectivity is controlled by the cyclization step. Bispropargyl methanes and amines have characteristics comparable to those of the ethers, and we predict that their selectivity will be dictated by their relative  $pK_a$ 's. Predictions for sulfone based on relative activation barriers were compared to the predictions based on relative  $pK_a$ 's so that the results can be easily verified by future experiments.

In conclusion, the mechanism of the Garratt–Braverman cyclization varies among the various bispropargyl substrates (Scheme 4). Selectivity can be induced by suitable unsymmetrical substitution of the substrates. The selectivity-determining step is different for sulfones and ethers: cyclization is the selectivity determining step for sulfones, while the rate of

**Scheme 4. [4 + 2] Cycloaddition (top) and Diradical (bottom) Pathways for the Base-Mediated GB Cyclization of Bispropargyl Systems, Where Bispropargyl Ether, Amine, and Methane Prefer the IMDA Pathway, whereas Bispropargyl Sulfone Prefers for the Formation of the Final Product**



isomerization determines the selectivity for ethers. In ether-like substrates, we predict selectivity from a simple calculation of  $pK_a$ , rather than the extensive study of the reaction mechanism.

## ■ ASSOCIATED CONTENT

### 📄 Supporting Information

The Supporting Information is available free of charge on the ACS Publications website at DOI: 10.1021/acs.joc.6b01053.

All the relevant tables and figures, along with the Cartesian coordinates of the optimized geometry (PDF)

## ■ AUTHOR INFORMATION

### Corresponding Author

\*E-mail: [anoop@chem.iitkgp.ernet.in](mailto:anoop@chem.iitkgp.ernet.in)

### Notes

The authors declare no competing financial interest.

## ■ ACKNOWLEDGMENTS

We acknowledge financial support from the Department of Science and Technology, New Delhi, in the fast track scheme to AA, and the computational facility at the Department of Chemistry supported by a DST special grant. S.J. is grateful to UGC, Government of India, for a fellowship. We acknowledge Surajit Nandi for a few urgent calculations to help with the revision.

## ■ REFERENCES

- (1) Garratt, P. J.; Neoh, S. B. *J. Am. Chem. Soc.* **1975**, *97*, 3255.
- (2) Garratt, P. J.; Neoh, S. B. *J. Org. Chem.* **1979**, *44*, 2667.
- (3) Braverman, S.; Segev, D. *J. Am. Chem. Soc.* **1974**, *96*, 1245.
- (4) Braverman, S.; Zafrani, Y.; Gottlieb, H. E. *Tetrahedron Lett.* **2000**, *41*, 2675.
- (5) Basak, A.; Das, S.; Mallick, D.; Jemmis, E. D. *J. Am. Chem. Soc.* **2009**, *131*, 15695.

(6) Maji, M.; Mallick, D.; Mondal, S.; Anoop, A.; Bag, S. S.; Basak, A.; Jemmis, E. D. *Org. Lett.* **2011**, *13*, 888.

(7) Mukherjee, R.; Mondal, S.; Basak, A.; Mallick, D.; Jemmis, E. D. *Chem. - Asian J.* **2012**, *7*, 957.

(8) Mondal, S.; Basak, A.; Jana, S.; Anoop, A. *Tetrahedron* **2012**, *68*, 7202.

(9) Ghosh, D.; Jana, S.; Panja, A.; Anoop, A.; Basak, A. *Tetrahedron* **2013**, *69*, 8724.

(10) Mitra, T.; Jana, S.; Bhattacharya, P.; Khamrai, U. K.; Anoop, A.; Basak, A.; Pandey, S. *J. Org. Chem.* **2014**, *79*, 5608.

(11) Das, J.; Mukherjee, R.; Basak, A. *J. Org. Chem.* **2014**, *79*, 3789.

(12) Schaefer, A.; Horn, H.; Ahlrichs, R. *J. Chem. Phys.* **1992**, *97*, 2571.

(13) Grimme, S.; Antony, J.; Ehrlich, S.; Krieg, H. *J. Chem. Phys.* **2010**, *132*, 154104.

(14) Eichkorn, K.; Weigend, F.; Treutler, O.; Ahlrichs, R. *Theor. Chem. Acc.* **1997**, *97*, 119.

(15) Goerigk, L.; Grimme, S. *Phys. Chem. Chem. Phys.* **2011**, *13*, 6670.

(16) Perdew, J. P.; Wang, Y. *Phys. Rev. B: Condens. Matter Mater. Phys.* **1992**, *45*, 13244.

(17) Chen, W. - C.; Chang, N. - Y.; Yu, C.-H. *J. Phys. Chem. A* **1998**, *102*, 2584.

(18) Becke, A. D. *J. Chem. Phys.* **1993**, *98*, 5648.

(19) Stephens, P. J.; Devlin, F. J.; Chabalowski, C. F.; Frisch, M. J. *J. Phys. Chem.* **1994**, *98*, 11623.

(20) Weigend, F.; Häser, M.; Patzelt, H.; Ahlrichs, R. *Chem. Phys. Lett.* **1998**, *294*, 143.

(21) Zhao, Y.; Truhlar, D. G. *Theor. Chem. Acc.* **2008**, *120*, 215.

(22) Becke, A. D. *Phys. Rev. A: At., Mol., Opt. Phys.* **1988**, *38*, 3098.

(23) Perdew, J. P. *Phys. Rev. B: Condens. Matter Mater. Phys.* **1986**, *33*, 8822.

(24) Tomasi, J.; Persico, M. *Chem. Rev.* **1994**, *94*, 2027.

(25) Cramer, C. J.; Truhlar, D. G. *Chem. Rev.* **1999**, *99*, 2161.

(26) Orozco, M.; Luque, F. J. *Chem. Rev.* **2000**, *100*, 4187.

(27) Tomasi, J.; Mennucci, B.; Cammi, R. *Chem. Rev.* **2005**, *105*, 2999.

(28) Orca 2.9.1, developed by Frank Neese, Max Planck Institute for Bioinorganic Chemistry, Muelheim/Ruhr, Germany.

(29) Ho, J.; Coote, M. L. *Theor. Chem. Acc.* **2010**, *125*, 3.

(30) Fraser, R. R.; Bresse, M.; Mansour, T. S. *J. Chem. Soc., Chem. Commun.* **1983**, *11*, 620.

(31) We have considered four plausible pathways: (a) diradical cyclization of bispropargyl, (b) anionic IMDA of bispropargyl anion, (c) IMDA of allenyne, and (d) diradical cyclization of bisallene. Pathways a and b demand high activation energies for the cyclization (see Scheme S1 in the Supporting Information), and hence, we proceeded with the mostly known pathways c and d.

(32) Kobychev, V. B.; Vitkovskaya, N. M.; Klyba, N. S.; Trofimov, B. A. *Russ. Chem. Bull.* **2002**, *51*, 774.

(33) Jana, S.; Anoop, A. *Phys. Chem. Chem. Phys.* **2015**, *17*, 29793.